

GT2010-888( \$

## "ONLINE THROUGHFLOW" – AUTOMATIC SIMULTANEOUS SIMULATION OF AN AXIAL FLOW TURBINE

Norbert Schinko\*, Martin Marx\*, Martin G. Rose\*, Stephan Staudacher\*,  
Jochen Gier\*\*, Norbert Hübner\*\*

\* Institute of Aircraft Propulsion Systems  
Stuttgart University  
Pfaffenwaldring 6  
70569 Stuttgart, Germany  
Email: norbert.schinko@ila.uni-stuttgart.de

\*\* MTU Aero Engines GmbH  
Dachauer Strasse 665  
80995 München

### ABSTRACT

A new turbine rig analysis method has been developed at the Institute of Aircraft Propulsion Systems (ILA) at Stuttgart University. This technique is known as "Online Throughflow" and involves the optimized adjustment of the input parameters of a Throughflow Method. The calculation is run whilst the turbine is being tested, achieving a match to measured data in about five minutes. The match between predicted and measured data is expressed as a chi-squared value. This provides a target parameter for a linear optimization procedure. Measured parameters such as inter-row static pressures, torque, mass-flow and rotational speed are used in this context. Input parameters such as row deviation and row loss are adjusted to give an optimized turbine simulation in close to real time.

Less than five minutes after taking a data scan of the experimental parameters at inlet to exit from and within the turbine, a converged simulation of the turbine is available. This simulation evaluates many other parameters within the turbine that are not directly measured, e.g. circumferential exit flow angles for all rows of aerofoils. Furthermore the single values of chi-squared from every measured variable can be used to decide if there is an error in the individual measurements.

The complete optimizer is programmed in LabView® and is integrated into the data acquisition system of the two-stage "Advanced Turbine Research and Demonstration Rig" (ATRD-Rig), which has been developed in a cooperation of ILA and the MTU Aero Engines (MTU). The testbed, as well as the instrumentation of the specific specimen from which all measurement values for the optimization have been taken, will additionally be described in the paper.

### ABBREVIATIONS

ADP Aerodynamic Design Point  
ATF Altitude Test Facility

ATRD	Advanced Turbine Research and Demonstration
ATRD-Rig	Advanced Turbine Research and Demonstration test carrier
C	identifier for static pressure tapings on the annulus casing
CAD	Computer Aided Design
CAM	Computer Aided Manufacturing
CFD	Computational Fluid Dynamics
CC	identifier for static pressure tapings inside the annulus casing cavities
cf.	confer
CH	identifier for static pressure tapings inside the hub cavities
cp.	compare
CPU	Central Processing Unit
Fig.	Figure
Gb	Gigabyte
GHz	Gigahertz
GNA	Gauss-Newton-Algorithm
H	identifier for static pressure tapings on the hub
ILA	Institute of Aircraft Propulsion Systems
LPT	Low Pressure Turbine
Max.	maximum
Min.	minimum
MP	measurement plane
MTU	MTU Aero Engines
NASA	National Aeronautics and Space Administration
NGV	nozzle guide vane
PC	identifier for platform static pressure tapings on the annulus casing

PH	identifier for platform static pressure tappings on the hub
RAM	Random Access Memory
Re	Reynolds Number
RBR	rotor blade row
RPM	Revolutions Per Minute
S1	circumferential stream surface
S2m	meridional stream surface
SGV	Streamline Curvature Computer Program Code of MTU
Tab.	Table
TelNet	specific computer network protocol
TF	Throughflow
vs.	versus
ZME	central measuring unit of the ATF
1D, 2D, 3D	one, two, three dimensional

## SYMBOLS

<b>a</b>	throughflow input variable (vector)	
<b>H</b>	Enthalpy	[J/kg]
<b>i, j, r</b>	index variables	[ - ]
<b>J</b>	Jacobian Matrix (matrix)	
<b>k</b>	iteration counter	[ - ]
<b>L</b>	Loss	[ - ]
<b>m</b>	number of flow parameters	[ - ]
<b>Ma</b>	Mach Number	[ - ]
<b>n</b>	number of input variables	[ - ]
<b>P</b>	Pressure	[Pa, bar]
<b>r</b>	radial direction	[m]
<b>s</b>	step width	[ - ]
<b>T</b>	Temperature	[K]
<b>u</b>	circumferential direction	[°]
<b>Y</b>	physical flow parameter (vector)	
<b>z</b>	axial direction	[m]
$\chi^2$	sum of least square-errors	[ - ]
$\Pi$	Pressure Ratio	[ - ]
$\sigma$	standard deviation (vector)	

## SUBSCRIPTION

,	subscript separator
is	isentropic
LIN	linearized value
M	measured value
s	static value
SL6	streamline 6 (meridional streamline)
t	total value
TF	Throughflow value
V1	Vane 1
V2	Vane 2

## SUPERSCRPTION

®	sign for legally protected products
*	normalized value
T	transposed matrix

## INTRODUCTION

Over the past two decades the operators of aero-engine gas turbines have demanded significant improvements. These improvements have included reliability, cost, environmental friendliness and above all reduced fuel consumption [1]. Steffens and Walther [2] state that these requirements can only be met with a consecutive development of new technologies and a quick realization of the resultant technical expertise gained in to the series production. The engine development activity requires both: computational simulation to support design and rig testing to confirm technological development. Before a complete prototype engine test can be performed, several tests of the individual engine components have to be carried out first. Low Pressure Turbine (LPT) rig tests, with the LPT as an example of a component of a gas turbine, include a high standard of instrumentation. At ILA such LPT test rigs are installed in one of the test cells of the Altitude Test Facility (ATF). This allows the adjustment of turbine inlet and exit conditions over a very wide range, simulating surrounding aero-engine components, from idle to take-off overall operating state. An adjustable water-brake is used to absorb the power of the turbine. In Fig. 1 the ATRD-Rig can be seen, mounted at the ATF.

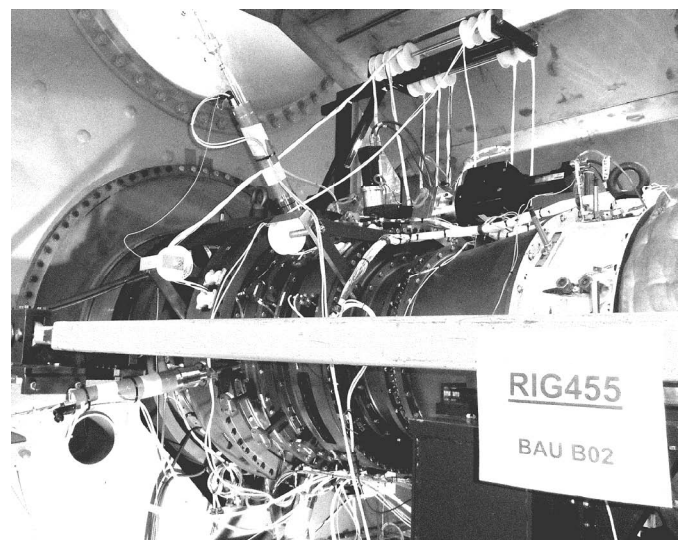


**Fig. 1: Picture of the ATRD-Rig mounted at the ATF of Stuttgart University**

The data acquired from the test rig is first displayed numerically and then visualized in various diagrams. This allows for the conventional control and monitoring of the facility and the turbine rig. The experimental data is also stored on the hard disks of the data acquisition system and can be used for subsequent “Offline” analysis. In Fig. 2 the established use of measurement data of a turbine rig test is presented in a schematic sketch. During the ATRD rig test for the first time the data is also made available to support the convergence of a two dimensional Throughflow (TF) simulation of the turbines internal flow. This process is called “Online Throughflow”.

There are a number of publications in which the principle of an “Online” simulation is described (cp. [3], [4], [5] and [6]). These references address the simultaneous simulation of whole engine behaviour using high level models during testing. There are major advantages with these kinds of performance simulations.

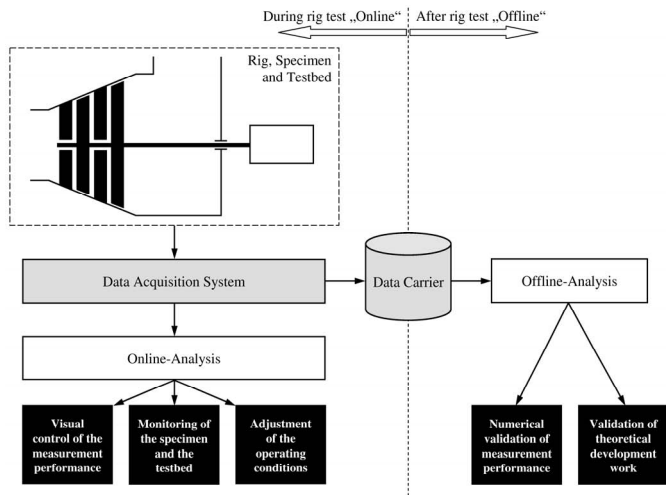


**Fig. 2: Schematic sketch of the established use of measurements of a turbine rig test**

The results are available without delay, whilst the test is still ongoing. This facilitates a much more detailed understanding of the behaviour of the machine and allows the adjustment of the testing procedure and the instrumentation for an improved and more detailed study of the performance parameters of the engine. The differences between simulation and measured data is also used to give a first warning in terms of instrumentation failures, thus allowing for rectification and the avoidance of losing test time.

In spite of the rapid development of computer technology a fully instationary three-dimensional calculation of the flow field through a turbine is still much too time consuming for a reasonable matching to all measured variables via an iterative adaption process during a turbine rig test. Because of this fact a much quicker and less complicated method for calculating the flow has to be used. In Fig. 3 a scheme of a simplified standard design process of an axial turbomachine is presented, following Boyer [7] and Casey [8]. It can clearly be seen that the calculation of the flow field by the “quasi-3D” theory first presented by Wu [9] in 1952 is still used in this procedure. The development of this type of two dimensional stationary flow calculation over the past decades led to a sophisticated and fast method for designing annuli and blade rows of turbomachines via an iterative process that is characterized by a variation of the calculation input parameters [10]. For example the aerodynamic losses and deviations of the used profiles must be specified and input by the user when running a TF Calculation. This flow calculation method has already been used for Offline-Analysis in reference to turbomachine rig test data. In this case

the calculation was tried to be adapted to the measurements by a semi automatic variation of the input parameters, as mentioned in a technical paper from Rose et al. [11]. The results were then used to evaluate non measured and not measurable values, which helped to validate the performance of the tested machine.

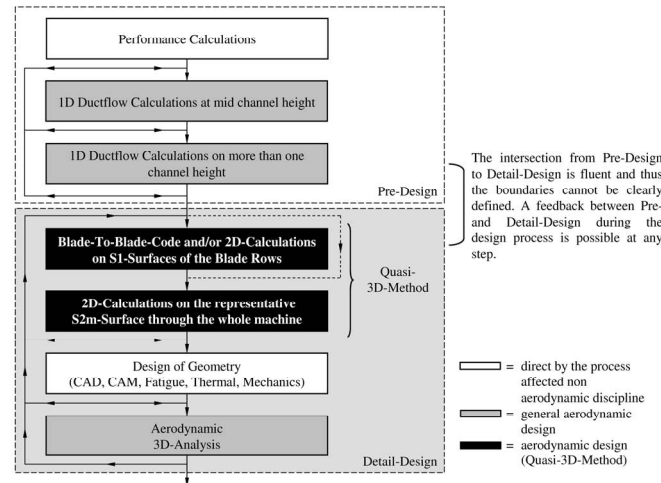


**Fig. 3: Schematic sketch of a typical, simplified aerodynamic design process of an axial turbomachine (cf. [7] and [8])**

For that reasons an existing two dimensional TF Calculation of the ATRD turbine, based on a streamline curvature computer code (SGV) provided by MTU [12], was introduced into a data acquisition system, which was set up for the rig tests in regard to the ATRD project. The developed optimizer provides the possibility to automatically adjust the TF calculation of the aerodynamic design point (ADP) of the test turbine, by a variation of the code input parameters, whilst keeping the turbine geometry fixed. As a result the solution closely approaches the measurements in every defined calculation plane. This process can be started directly after finishing a data scan during the rig test and the results of the converged TF Calculation can be directly displayed on the monitors of the data acquisition system. The optimizer was also developed to be used for other turbine rigs including turbines with different numbers of stages. For future LPT rig tests at the ATF it is planned to include the method of TF matching consistently.

## DESCRIPTION OF THE TURBINE TEST RIG AND THE DATA ACQUISITION SYSTEM

For The Online Throughflow Method has been applied to an ATRD LPT rig test at ILA. The ATRD-Rig is a closed testbed including a turbine with aluminum blades. It was especially designed to simulate a two staged LPT at very low Reynolds conditions and to give a minimum overall power consumption during testing. This allows a maximum of running hours at minimum price for taking a large amount of measurement data and to get a fundamental understanding of the physics in the tested turbine at simulated high altitude. In

Tab. 1 the maximum operating range of the rig and the ADP of the tested specimen are listed. In Fig. 4 a layout drawing of the complete rig can be seen, which includes markings of the axial positions of the measurement planes (MP) with the gauges used to evaluate the turbine entry and exit conditions during testing. Furthermore it can be identified that the rig is divided into three sections: Rig-Inlet, LPT-Module and Rig-Exit.

	Unit	Max.	Min.	ADP
Massflow	kg/s	15	0.0	2.7
$T_t$ at Entry	K	400	280	350
$T_t$ at Exit	K	350	263	299
$P_t$ at Entry	bar	2.0	0.1	0.223
$P_t$ at Exit	bar	1.0	0.05	0.113
Rotational Speed	1/min	4000	0.0	3600
Power	kW	1200	0.0	137.0

**Tab. 1: Operating range of the Rig and ADP of the tested turbine**

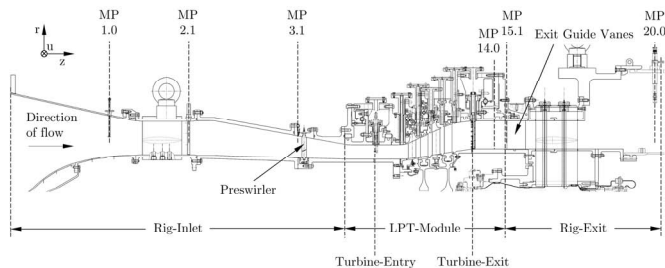


**Fig. 4: Layout drawing of the complete ATRD-Rig, including MP-Positions and sub-component descriptions**

**Rig-Inlet and Rig-Exit.** The instrumentation of Rig-Inlet and -Exit equates to the established technique to measure entry and exit conditions of turbine rigs [13]. The inlet total pressure of the airflow delivered from the ATF is measured at mid channel height via four total pressure probes equally arranged in circumferential direction in MP1.0. Inlet total temperature is measured in MP2.1 by eight rakes, each with three gauges equally radially spaced. With the static pressure measured in MP3.1 by 16 static pressure tapings at hub and casing inside the annulus and a loss value from a previous calibration of the Rig-Inlet duct, the total pressure at Turbine-Entry is evaluated. This correction takes the generated loss of the 120 vanes of the preswirl into account, which is used to simulate the flow of an in engine upstream blade row. The measured total temperature is assumed to be constant from MP2.1 to Turbine-Entry. In MP15.1 the total exit pressure is measured by kielheads mounted at the leading edges of three of the 58 exit guide vanes at mid channel height, to monitor the exit conditions in combination with three temperature measurements in MP20.0.

**LPT-Module.** The LPT-Module is the central unit of the ATRD-Rig. Inside this part of the test carrier the flow at Turbine-Entry and Turbine-Exit, as well as between the blade rows is quantified by probes, kielheads mounted on the nozzle

guide vanes (NGV), rakes and pressure tapings at the static part of the annulus. For a better understanding of the description of the LPT-Module instrumentation a corresponding layout drawing is presented in Fig. 5. The layout includes, as in to Fig. 4, markings of the axial positions of the measurement planes, which are perpendicular to the z-axis of the mapped coordinate.

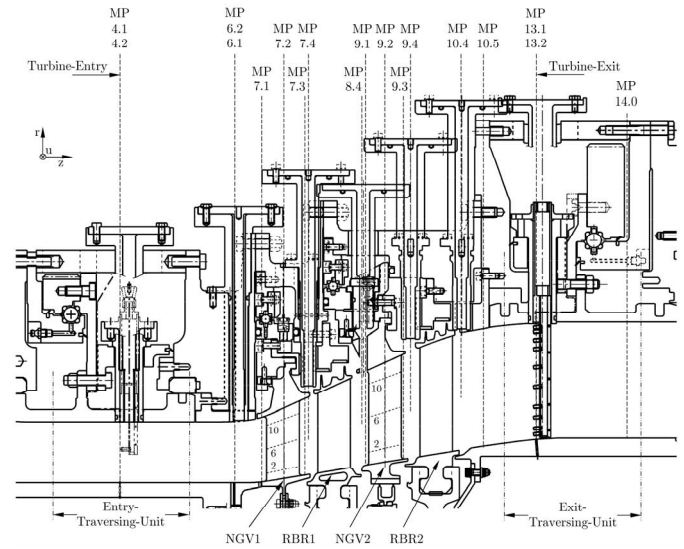


**Fig. 5: Layout drawing of the LPT-Module, including MP-Positions and sub-component descriptions**

**Devices for traversing probes.** Altogether the rig provides 26 access devices for traversing probes with a maximum shaft diameter of ten millimeters. Each of the two Traversing Units at Turbine-Entry and -Exit can be moved in circumferential direction by a servo motor. Inside the Exit-Traversing-Unit there are three additionally implemented total pressure rakes and three total temperature rakes with ten gauges each, to get a representative measurement of the turbine exit conditions. The remaining probe access devices are fixed relative to the casing. Here the effect of an area traverse is caused by a rotation of the NGVs, where each row is driven by a servo motor. During the measurement campaign some of the access devices were used for area traverses with pneumatic fivehole and two dimensional hotfilm probes, which were mounted in stepper motor probe adjustment devices. A detailed description of the rig possibilities in terms of adjustable probe measurement and the technique used to evaluate the fivehole probe data is described in [14].

**Installed fixed measurements.** Tab. 2 includes all axial positions of static pressure tapings and the number of tapings per type. The character C identifies gauges at the annulus casing, H at the hub. The combination PC marks tapings on the NGV platforms at casing side, PH platform statics at hub side. CC labels statics inside the casing cavities and CH statics inside the cavities on the hub-side. The given gauges per chart item are equally distributed in circumferential direction, except of the platform statics of MP7.3, MP9.1 and MP9.3. These are

each arranged across one blade pitch for an accurate average value of the static pressure at NGV hub and tip per MP. Some NGVs have additional static pressure tapplings along streamlines (see identifier 2, 6 and 10 in Fig. 5) of profile pressure or suction side.

	C	H	PC	PH	CC	CH
MP4.1	8	8	-	-	-	-
MP6.1	4	4	-	-	-	-
MP7.1	-	-	3	3	-	-
MP7.3	-	-	10	10	3	3
MP9.1	-	-	10	10	3	3
MP9.3	-	-	10	10	3	3
MP10.5	3	3	-	-	-	-
MP13.1	6	6	-	-	-	-
MP14.0	3	3	-	-	-	-

**Tab. 2: Static pressure tapplings of the LPT-Module in the range of annulus casing and hub**

Together with the measurements of kielheads, which are mounted at the leading edges of the NGVs in MP7.1 and MP9.1 at the heights of the streamlines, the velocity profiles of the NGVs can be evaluated and displayed at three channel heights.

In addition to the described instrumentation there exist three more measurements that are essential to converge the TF Calculation to an operating point of the turbine. The rotational speed of the rotor and the torsional moment of the rotor shaft are measured by a torque tube with high accuracy and represent the generated mechanical power of the turbine. The massflow through the turbine is evaluated with the help of a calibrated venturi nozzle, placed in the plumbing of the ATF upstream of the rig and right after a plenum chamber. This chamber is used to measure the static fluid properties needed for the calculation of massflow.

Other installed measurements are required for safety and monitoring issues during testing and are not needed for the Online Throughflow. Because of this fact they are not described in this paper. For a more detailed description of the rig instrumentation [13] can be taken as a reference.

**Data acquisition system.** The data acquisition system for the ATRD measurement campaign is programmed in LabView® on the basis of an upgradeable composition of computers (3GHz Dual Core, 4Gb RAM) set up with Windows XP®. In Fig. 6 the arrangement of the participating subsystems is shown.

Pressures, Temperatures and other digital channels are measured with an actualization rate of 4Hz by the Central Measuring Unit of the ATF named ZME and provided as digital values in scientific standard units by the “Verse-PC” over an Ethernet port. The overall ATRD-System consists of four computers with different tasks each. The “Interface-Computer” obtains the pure measurements, produces resultant averaged values for the MPs and calculates the basic performance parameters of the whole machine. For these calculations humidity is taken into account by an implemented chart based

fluid model, generated with a free distributable computer program of NASA [15].

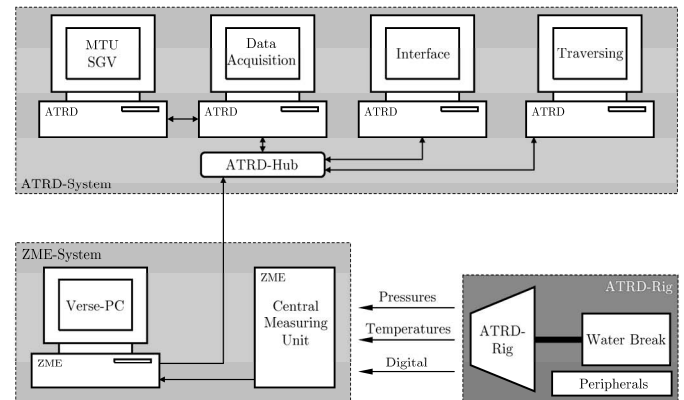


**Fig. 6: Arrangement of the involved subsystems in terms of data acquisition and evaluation**

Isentropic calculations are done in accordance to a proposal of Kurzke [16], to guarantee a maximum of accuracy for the evaluated performance parameters. All produced values are provided via Ethernet for the other subsystems. The “Traversing-Computer” takes care of the probe measurement evaluation and visualization, the positioning of the traverse probes and the storage of these results. A set of time averaged measurement and performance data can be produced with the “Data Acquisition-Computer”. The resultant values can be stored, displayed numerically or in graphs and used to converge the TF to the measurements. A more detailed description of the ATRD data acquisition system and the used calculation methods for the performance parameters can be found in [13].

## DESCRIPTION OF THE TECHNIQUE USED TO MATCH THROUGHFLOW CALCULATIONS AND THE MEASUREMENT DATA

The matching process of a TF calculation to the measured rig test data requires the use of a numerical optimization routine. The TF as an industrial code is only available as a “black box”, which means without knowing the source code in detail. The TF and the developed optimizer sub routine of the “Data Acquisition System” are furthermore running on different computers of the same type, thus the latter has to incorporate a communication routine to remote control the TF machine. This communication is fully automated using the Telnet® Protocol [17]. The optimizer routine permanently produces text based input files for the TF, transfers them to the “MTU SGV-Computer”, runs the calculation via Telnet Remote Commands, waits for the calculation to be finished and then uses the results for producing a further, better adapted set of TF input data. After having reached a satisfying grade of optimization, the results of the TF calculation can be displayed and evaluated.

**Input variables and optimization parameters.** The input data set to be optimized is defined by several variables, which are specified directly in the input file of the throughflow solver.

Those are for instance the turbine inlet total pressure, the inlet total temperature, the mass flow, the rotational speed, the blade exit angles and the row loss coefficients. As a result of the TF calculation, up to about 30 matching parameters are read out of the TF result file using a parser routine, each of one representing a specific physical value within the turbine flow field to be matched with the measured data. This data contains inlet conditions, turbine performance data (power, efficiency) as well as inter-row total and static pressures at hub and casing inside the annulus. The optimizer has to calculate the best input variable set to match the resultant TF parameters to the measured ones as closely as possible.

**Optimization algorithm.** For the optimization the gradient based Gauss-Newton-Algorithm (GNA), a weighted Non Linear Least Squares Algorithm, was chosen. The objective function of the optimization, thus the correlation between input variables and result parameters, is represented by the TF solution and can therefore not be expressed analytically. The basis of the Least Squares Method is the  $\chi^2$ -value

$$\chi^2 = \sum_{i=1}^m \frac{(Y_{LIN,i} - Y_{M,i})^2}{\sigma_i^2} \quad (1)$$

which represents the squared sum of the residuals of the TF results ( $Y_{TF}$ ) compared to the  $m$  measured values ( $Y_M$ ). The  $\chi^2$ -value is normalized by the standard deviation of the measured values ( $\sigma_i$ ) and can be seen as the indicator of the goodness of optimization that has to be minimized to obtain optimum results. Since the TF solution can be considered being nonlinear, it is linearized with respect to changes to the input variables  $a_j$ , thus

$$Y_{LIN,i} = Y_{TF} + \Delta a_1 \frac{\partial Y_{TF,i}}{\partial a_1} + \dots + \Delta a_n \frac{\partial Y_{TF,i}}{\partial a_n}, \quad i = 1..m \quad (2)$$

Expressed in a matrix scheme using the Jacobian Matrix

$$\mathbf{J} = \begin{bmatrix} \frac{\partial Y_{TF,1}}{\partial a_1} & \frac{\partial Y_{TF,1}}{\partial a_2} & \dots & \frac{\partial Y_{TF,1}}{\partial a_n} \\ \frac{\partial Y_{TF,2}}{\partial a_1} & \frac{\partial Y_{TF,2}}{\partial a_2} & \dots & \frac{\partial Y_{TF,2}}{\partial a_n} \\ \vdots & \vdots & \ddots & \vdots \\ \frac{\partial Y_{TF,m}}{\partial a_1} & \frac{\partial Y_{TF,m}}{\partial a_2} & \dots & \frac{\partial Y_{TF,m}}{\partial a_n} \end{bmatrix}, \quad (3)$$

$\chi^2$  can be expressed as

$$\begin{aligned} \chi^2 &= \sum_{i=1}^m \frac{\left( Y_{TF,i} - Y_{M,i} + \sum_{j=1}^n [J_{ij} \Delta a_j] \right)^2}{\sigma_i^2} \\ &= \sum_{i=1}^m \frac{(Y_{TF,i} - Y_{M,i} + \mathbf{J}_i \Delta \mathbf{a})^2}{\sigma_i^2} \end{aligned} \quad (4)$$

As illustrated in [18], introducing the normalization

$$\mathbf{J}^* = \left[ \frac{1}{\sigma_1}, \dots, \frac{1}{\sigma_m} \right] \mathbf{J} \quad (5)$$

and the condition to minimize  $\chi^2$

$$\frac{\partial \chi^2}{\partial \Delta a_r} = 0, \quad r = 1..n \quad (6)$$

leads to a linear system of  $n$  equations

$$\mathbf{J}^{*T} \mathbf{J}^* (\mathbf{a}^{(k+1)} - \mathbf{a}^{(k)}) + \mathbf{J}^{*T} \frac{\mathbf{Y}_{TF} - \mathbf{Y}_M}{\boldsymbol{\sigma}} = 0 \quad (7)$$

that solves the least squares optimization problem [19]. Starting from an initial input variable set  $\mathbf{a}^{(k=1)}$ , iterative solving of these equations leads to an optimized input variable set  $\mathbf{a}^{(k+1)}$ . Mathematically, the optimization is achieved by changing the input variables in the direction of the calculated Jacobian Matrix, which equals the first derivative of the objective function. Since there is no analytical objective function, the Jacobian Matrix has to be calculated numerically using the Finite Differences Method. Besides the start solution, for each column of the Jacobian one TF calculation has to be done. That means, for  $n$  Parameters at least  $n+1$  TF calculations have to be done to obtain the next input variable set.

**Special requirements for the TF Optimization.** The local Gauss-Newton-Method is a quick and stable optimization method as long as a good initial solution is known. For this application the initial input variable vector can be obtained from preliminary design and CFD data which proved to fit well enough to not cause any convergence problems of the optimization. Nonetheless the GNA had to be adapted to meet some special requirements of the TF Solver. The optimizer is a purely mathematical tool which does not check the physical plausibility of the input parameters. Unfeasible input data can lead to a non-converged, erroneous TF solution, sometimes even to no solution at all. The convergence behavior of the TF is not predictable, slight changes in the input data set can cause the TF to not converge and give out errors. This TF can therefore be seen as an erratic objective function with discontinuities that has to be optimized. The typical GNA is not able to optimize discontinuous functions. The convergence of every single TF calculation therefore has to be checked automatically, and a strategy is implemented to overcome unfeasible TF solutions. To meet these requirements, the optimizer was modified to cope with discontinuities in the solution space by applying an under-relaxation and a Line-Search approach. An illustration of this approach is given in Fig. 7. After calculating the Jacobian Matrix, the system of equations is resolved to obtain the new input variable vector  $\mathbf{a}^{(k+1)}$ . Unlike the normal GNA optimization does, this vector is not directly chosen for the next iteration, and is therefore called the theoretical new input vector. Along the direction of this theoretical vector about 20 to 30 different step widths are calculated, leading to a set of possible next vectors. The vector

with the lowest  $\chi^2$ -value is then chosen as real new input variable vector  $a^{(k+1)}$  for the next iteration. Following this strategy, the optimizer is not affected by discontinuities as long

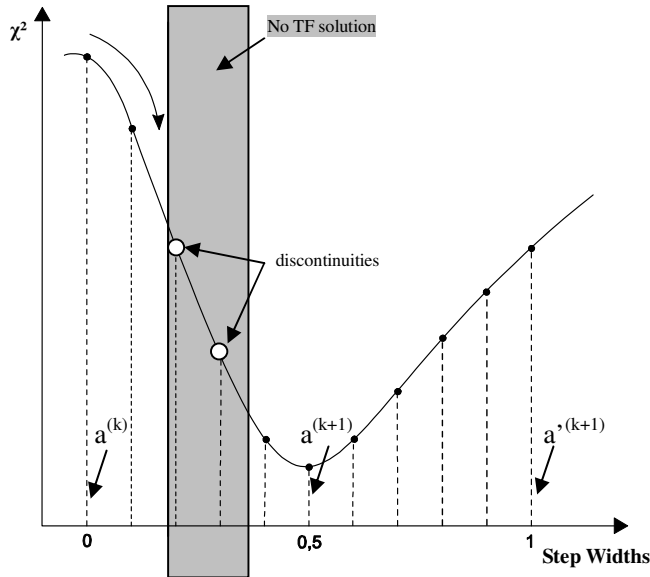


**Fig. 7: Line-Search-Approach to overcome areas of TF-discontinuity**

as at least one feasible solution is found among the calculated step widths. During Line Search, again every single point calculated needs a TF calculation to be run. Thus the overall calculation time increases, but enables the optimizer to get a solution with almost no constraint to TF convergence. The whole optimization routine including the Line Search Algorithm is presented in Fig. 8.

## DISCUSSIONS AND RESULTS

**Optimizer comparison.** The introduced GNA is a local, gradient-based optimization technique. Like other local optimization methods, it can neither guarantee convergence nor finding a global optimum solution. The underlying optimization problem can be addressed with many different optimization techniques. For the evaluation of the most capable algorithm, a preliminary study using different optimization techniques was performed, particularly to compare several local and global optimization routines. Global optimization techniques like Genetic Algorithms address the whole solution space at once, using heuristical methods to find minima or maxima. Their chance of finding global optimum is better, but the enormous calculation time disqualifies them for online analysis. This statement could be proved, as the results showed the GNA being the best local optimizing algorithm for the introduced problem with only a couple of minutes of calculation time. The reached level of adaption can only be beaten by Global Genetic Algorithms which would therefore need a couple of days of calculation time to obtain a slightly better result.

**Online capability.** Due to the fast calculation time of the algorithm the optimization process does not take longer than 5 minutes, which allows an online analysis during the rig test.

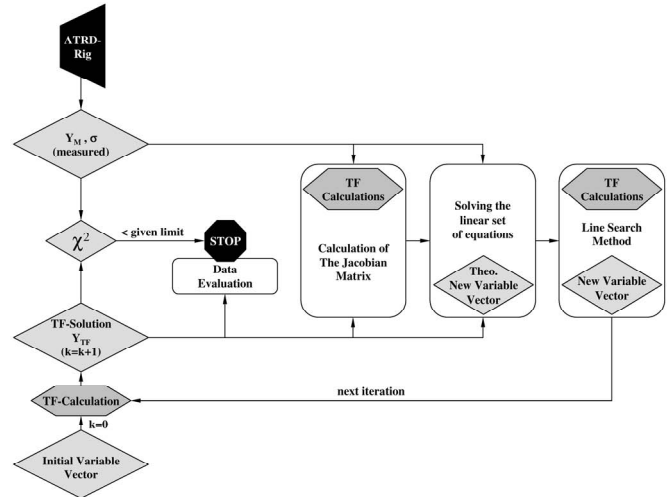


**Fig. 8: Optimization scheme including the Line-Search-Method**

About 95% of this whole optimization time is needed for converging the TF code, which leaves only about 5% for the mathematical optimization. Into the communication routine to run the TF solver there is included a stacking system for full parallelization ability, which is significantly reducing the minimum possible optimization time. In fact, the time is only limited by the amount of CPUs installed at the TF machine. With today's standard high level computer technology and the use of the optimizer's stacking system, a calculation time of less than one minute could be practically achieved.

**Optimized characteristic.** During rig test, the optimizer was used to create a TF solution for every operating point of the turbine characteristic. The ADP was optimized based on a preliminary ADP input file which was used during turbine design. The following off-design points were then optimized using this ADP solution. The characteristic contains four different rotational speed lines. Having performed the optimization for every running point of the characteristic, the TF result data can be plotted against the measured values to investigate the plausibility of the optimization results. In Fig. 9 a comparison of the enthalpy drop over pressure ratio is presented for four different rotational speeds, where the solid lines represent the measured values and the dashed lines the corresponding optimized TF calculation results. It has to be mentioned that the TF was not converged on turbine power as an input parameter, but only the surrounding conditions as well as flow angles and loss coefficients. The mean overall level of  $\chi^2$  after each optimization is about unity, indicating that the remaining mean error of each parameter is about the size of its standard deviation.

**Comparison of Mach Numbers and Flow Angles.** In Figs. 10 and 11 plots of the mid-height isentropic Mach

Numbers of vane 1 and vane 2 are presented. The isentropic Mach Numbers were calculated out of the measured total and static pressure up- and downstream the vanes.

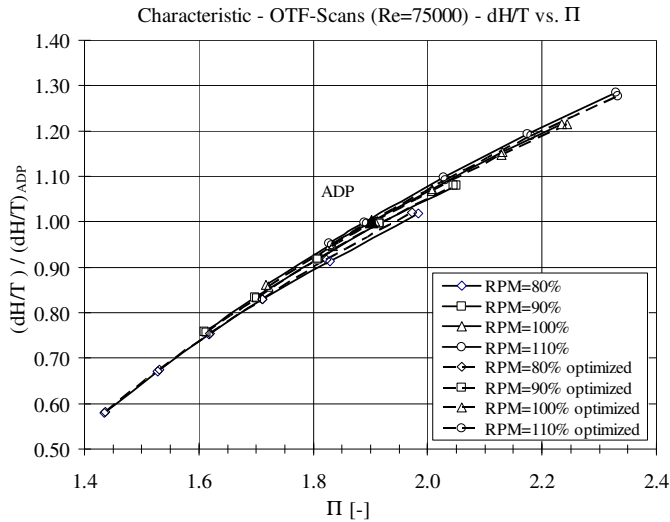


**Fig. 9: Comparison of TF results to measured values using the dH/T-Characteristic**

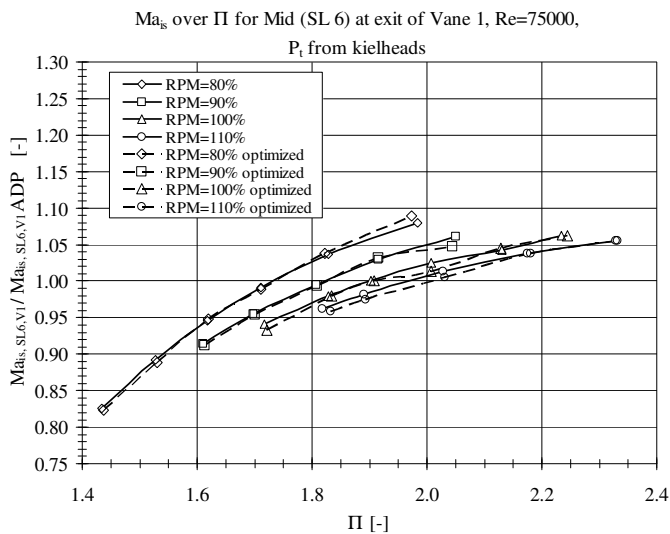


**Fig. 10: Isentropic Mach Number vs. Pressure Ratio at Vane 1**

At Vane 1, the level of agreement of the optimized solution is very high. At Vane 2, there can be noticed an almost constant offset of the TF Mach Number. This offset is caused by the total pressure at inlet of Vane 2 being about 2% too low, compared with the measured data. A possible explanation to this pressure mismatch, which occurred in every optimized TF solution, is unsteady static pressure interaction of the Vane 2 flow field due to the probe position being right on the leading edge. Also rotor leakage effects and Vane 1 wake interactions can lead to this offset. In both figures it can be further seen that the optimized solutions fluctuate around the measured solution, which can be

explained by differing solutions due to local minima which can not be avoided.

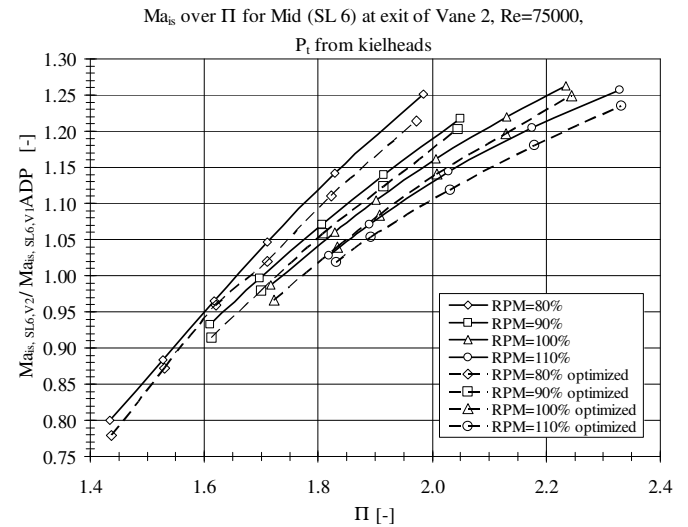


**Fig. 11: Isentropic Mach Number vs. Pressure Ratio at Vane 2**

In Figs. 12 to 15 the optimized tangential flow exit angle and Mach Number distributions of the second blade and vane row are presented and compared with the respective flow angle and Mach Number data obtained by area traversing using fivehole probe data. Since the TF is a two dimensional code, it is not capable of resolving secondary flow effects in detail. This is one reason that causes the optimized pressure distribution to differ close to the hub and casing walls. Another effect that is strongly influencing the flow field especially close to the hub wall is flow leakage. Flow leaving and entering the channel through the seals is causing the fluid inside to change direction and influences the total pressure. This effect cannot be resolved by the TF, which lead to the large differences visible at the hub of Vane 2 and particularly in the angle profile of Rotor 2, where the large wall offset even causes the mid-height angles to differ due to the mass flow integration of the TF code.

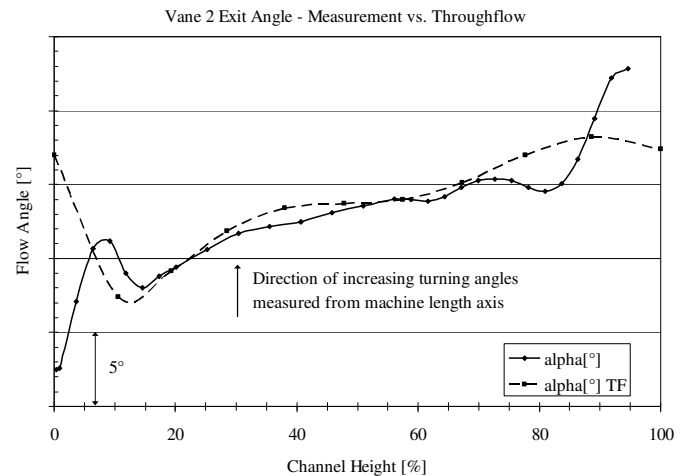


**Fig. 12: Flow angles at exit of Vane 2, ADP**

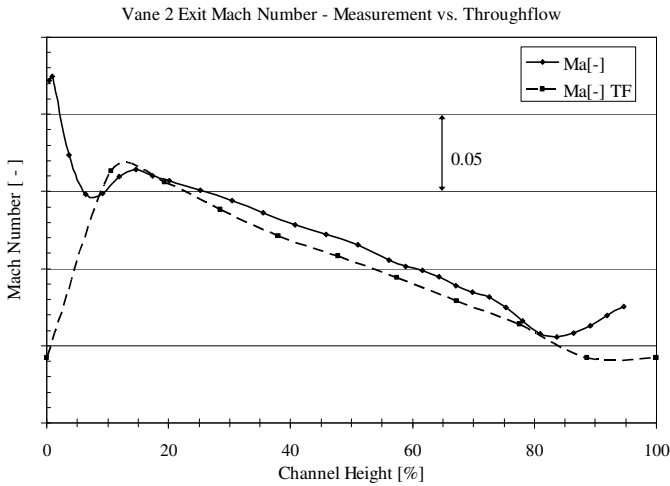


Fig. 13: Mach Numbers at exit of Vane 2, ADP

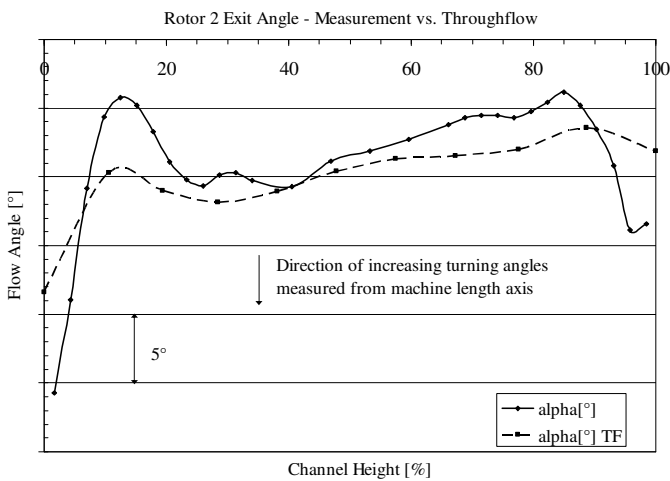


Fig. 14: Absolute flow angles at exit of Rotor 2, ADP

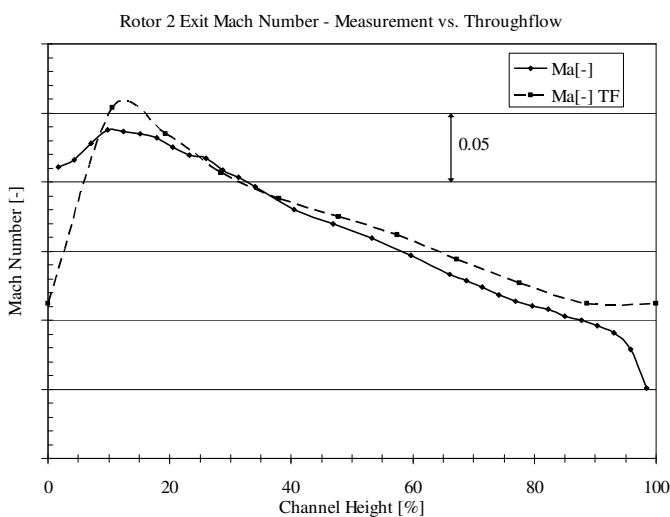


Fig. 15: Mach Numbers at exit of Rotor 2, ADP

An attempt was made to adapt the angular profile of Rotor 2 to meet the experiment, which led to a TF solution perfectly matching the measured angles, but with a large offset in turbine power and total pressure in that plane due to the model's lacking ability to resolve the wall effects sufficiently.

**Turbine Efficiency.** The level of agreement of the optimized characteristic is very satisfactory; however, there are some differences of the TF solution in terms of turbine efficiency. Throughout the characteristic a discrepancy of  $-1.1\%$  up to  $+0.6\%$  occurs. This can be due to the stated weaknesses of the TF model to resolve secondary flows and the leakage effects. However, the general level of confidence concerning efficiency calculation in the turbine rig is around  $0.8\%$ , which could additionally explain the mismatching efficiency values.

**Row Loss Calculation.** The TF optimization and matching allows the calculation of data which cannot or only intricately be measured in the turbine. A big advantage of Online TF optimization is the possibility to plot row loss coefficients for every operating point. In Fig. 16 the stagnation pressure loss coefficient [20] for Vane 2 is presented as a function of Isentropic Mach Number for two rotational speeds, 90% and ADP. This coefficient is defined as

$$L_{Pt} = \frac{P_{t,in} - P_{t,out}}{P_{t,out} - P_{s,out}} \quad (8)$$

For the ADP, the measured loss value obtained using five-hole probe data is also given. The optimized TF loss differs about 6% relative to the calculated value, which is less than 1% absolute. As inspected, the vane row loss from the converged TF rises with increasing vane exit isentropic Mach Number (Fig. 16).

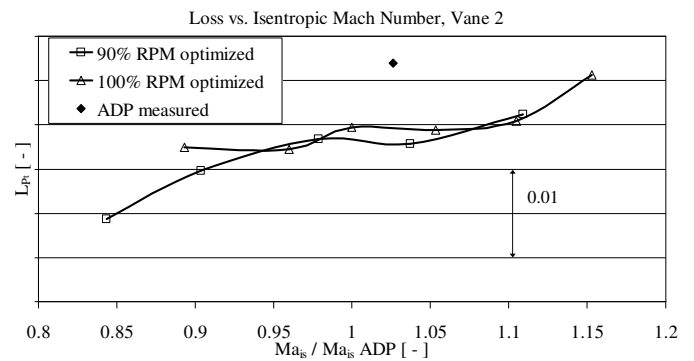


Fig. 16: Vane 2 Stagnation Pressure Loss vs. Isentropic Mach Number

## CONCLUSIONS

A new turbine rig analysis system has been developed and demonstrated at ILA named "Online Throughflow". This system allows automatic and simultaneous simulation of the turbine using a Throughflow Code during the test. The process involves the minimization of the chi-squared statistical variable using a gradient based optimization routine. The process was found to

be robust and, due to the full parallelization ability, run times of only a few seconds are possible with additional computational resources provided.

At convergence the optimized Throughflow solution offers a simulation of the flow physics inside the turbine. Variables that have not been measured are thus available to inform the test engineers of the nature of the flow. This allows an understanding of the evolution of parameters such as loss and deviation for all the individual components without the requirement to do detailed area traverses at every point.

Another major advantage of the Online Throughflow approach is that at convergence the chi-squared values for each variable indicate where residual errors lie. If a particular variable has a high chi-squared value we know that either the experimental values are misleading or that the Throughflow code has a lack of physical correctness in this area. A leaky static pressure tapping can be identified during the turbine run. Online Throughflow will thus lead to better tests and better simulation of turbines. In the future it is hoped that Online Throughflow will become a significant tool for the analysis of in engine data – giving improved understanding of the performance of the installed turbine.

## ACKNOWLEDGMENTS

The presented paper was developed in terms of the Advanced Turbine Research and Demonstration Project. This cooperation project between MTU and ILA was launched as a result of the Turbine Competence Centrum founded in 2006 between MTU and Stuttgart University. The authors would like to express their gratitude to the whole MTU Company for their support and the possibility to publish the gained know-how resulting from the cooperation project.

## REFERENCES

- [1] Broichhausen, K.; Wiedra, M.: “Steuerung komplexer Entwicklungskonzepte bei MTU Aero Engines”, Management von Innovation und Risiko, Teil IV: Steuerung risikoreicher Innovationsprojekte, Pages 285-299, 2. Edition, Springer-Verlag, Berlin 2006
- [2] Steffens, K.; Walther, R.: “Driving the Technological Edge in Airbreathing Propulsion”, AIAA Paper, 2003
- [3] Davis, J. et al.: “Model-Based Data Validation”, Proceedings of the Joint Technology Showcase on Integrated Monitoring, Diagnostics, and Failure Prevention, Mobile Alabama 1996
- [4] Malloy, D.J.; Chappell, M.A.; Biegl, C.: “Real-Time Fault Identification for Developmental Turbine Engine Testing”, ASME Turbo Expo, 97-GT141, Orlando 1997
- [5] Malloy, D.J.; Webb, A.T.; Kidman, D.S.: “MF-22/F119 Propulsion System Ground and Flight Test Analysis Using Modeling and Simulation Techniques”, ASME Turbo Expo, GT2002-30001, Amsterdam 2002
- [6] Bauer, M.: “Modulares Leistungsberechnungsverfahren zur automatisierten modellbasierten Leistungsanalyse von Gasturbinen”, PhD Thesis, Institute of Aircraft Propulsion Systems, Stuttgart 2005
- [7] Boyer, K.M.: “An Improved Streamline Curvature Approach for Off-Design Analysis of Transonic Compression Systems”, PhD Thesis, Virginia Polytechnic Institute and State University, Blacksburg Virginia 2001
- [8] Casey, M.V.: “Computational Methods for Preliminary Design and Geometry Definition in Turbomachinery”, Turbomachinery Design using CFD, AGARD-LS-195, Chapter 1, 22 Pages, London 1994
- [9] Wu, C.-H.: “A General Theory of Three-Dimensional Flow in Subsonic and Supersonic Turbomachines of Axial-, Radial and Mixed-Flow Types”, Technical Note 2604, National Advisory Committee for Aeronautics (NACA), Washington 1952
- [10] Hildebrandt, T.: “Weiterentwicklung von 3D Navier-Stokes-Strömungsrechnungsverfahren zur Anwendung in hochbelasteten Verdichter- und Turbinengittern”, PhD University of the Federal Armed Forces, Munich 1998
- [11] Rose, M.G.; Harvey N.W.; Seaman P.; Newman D.A.; McManus D.: „Improving the Efficiency of the Trent 500 HP Turbine using Non-Axisymmetric End Walls. Part II: Experimental Validation“, ASME Turbo Expo, 2001-GT-0505, New Orleans 2001
- [12] Dupslaff, M.; Paul, T.: “Eingabebeschreibung für das Stromliniengeometrieverfahren (SGV)“, Version 02.05.2007, MTU Aero Engines GmbH, Munich 2007
- [13] Saravanamutto, H.I.H.: “Recommended Practices for Measurement of Gas Path Pressures and Temperatures for Performance Assessment of Aircraft Turbine Engines and Components”, Report of the Propulsion and Energetics Panel Working Group 19, AGARD-AR-245, Essex 1990
- [14] Schinko, N.; Kürner M.; Staudacher S.; Rose M.G.; Gier J.; Raab I.; Lippl F.: “Das ATRD-Projekt – Ein Beispiel für die Zusammenarbeit von Industrie und Universität zur Förderung der Grundlagenforschung”, DGLR Congress, DLRK2009 121156, Aachen 2009
- [15] McBride, B.J.; Gordon, S.: “Computer Program for Calculation of Complex Chemical Equilibrium Compositions and Applications”, Part I & II, NASA Technical Report 1311, Ohio 1994, 1996
- [16] Kurzke, J.: “About Simplifications in Gas Turbine Performance Calculations”, ASME Turbo Expo, GT2007-27620, Montreal 2007
- [17] Dong, J.: “Network Protocols Handbook”, 4<sup>th</sup> edition, Javvin Technologies Inc., Saratoga 2007
- [18] Marx, M.: “Halbautomatisierte Optimierung von Turbinen-Throughflow-Berechnungen mit Hilfe der  $\chi^2$ -Methode auf Basis von Messdaten”, Diploma Thesis, Institute of Aircraft Propulsion Systems, Stuttgart, 2009
- [19] Å. Björck, Numerical Methods for Least Squares Problems, SIAM, 1996
- [20] Denton, J. D., 1993, "Loss Mechanisms in Turbomachines," ASME 93-GT-435